Environmental Science & Technology

Article

pubs.acs.org/est

A Time-Domain Nuclear Magnetic Resonance Study of Mediterranean Scleractinian Corals Reveals Skeletal-Porosity Sensitivity to Environmental Changes

Paola Fantazzini,*[,†,‡] Stefano Mengoli,[§] Stefania Evangelisti,[†] Luca Pasquini,[†] Manuel Mariani,[†,‡] Leonardo Brizi,[†,‡] Stefano Goffredo,[∥] Erik Caroselli,[∥] Fiorella Prada,[∥] Giuseppe Falini,[⊥] Oren Levy,[@] and Zvy Dubinsky[@]

[†]Department of Physics and Astronomy, University of Bologna, Viale Berti Pichat 6/2, 40127 Bologna, Italy

[‡]Centro Enrico Fermi, 00184 Roma, Italy

[§]Management Department, University of Bologna, Via Capo di Lucca 34, 40126 Bologna, Italy

[∥]Marine Science Group, Department of Biological, Geological and Environmental Sciences, Section of Biology, University of Bologna, Via F. Selmi 3, 40126 Bologna, Italy

[⊥]Department of Chemistry, "G. Ciamician", University of Bologna, Via F. Selmi 2, 40126 Bologna, Italy

[@]The Mina and Everard Goodman Faculty of Life Sciences, Bar-Ilan University, Ramat-Gan 52900, Israel

Supporting Information

ABSTRACT: Mediterranean corals are a natural model for studying global warming, as the Mediterranean basin is expected to be one of the most affected regions and the increase in temperature is one of the greatest threats for coral survival. We have analyzed for the first time with time-domain nuclear magnetic resonance (TD-NMR) the porosity and pore-space structure, important aspects of coral skeletons, of two scleractinian corals, *Balanophyllia europaea* (zooxanthellate) and *Leptopsammia pruvoti* (nonzooxanthellate), taken from three different sites on the western Italian coast along a temperature gradient. Comparisons have been made with mercury intrusion porosimetry and scanning electron microscopy images. TD-NMR parameters are sensitive to changes in the pore structure of the two coral species. A parameter, related to the porosity, is larger for *L. pruvoti* than for *B. europaea*, confirming previous non-NMR results. Another parameter representing the fraction of the pore volume with pore sizes of less than 10−20 μm is inversely related, with a high degree of statistical significance, to the mass of the specimen and, for *B. europaea*, to the temperature of the growing site. This effect in the zooxanthellate species, which could reduce its resistance to mechanical stresses, may depend on an inhibition of the photosynthetic process at elevated temperatures and could have particular consequences in determining the effects of global warming on these species.

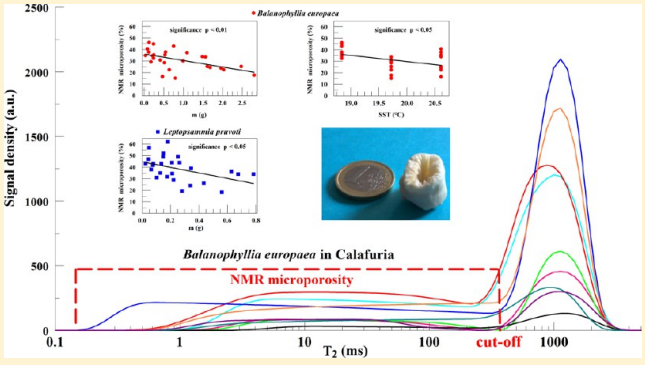

INTRODUCTION

Corals and Global Warming. Global climate change is the defining environmental issue of our times and is expected to profoundly affect all levels of ecological hierarchies and a broad array of terrestrial and marine ecosystems.[1−5] Marine communities are expected to be affected more than terrestrial ones by the effects of climate change,[6] especially in temperate areas.[7] Thus, the Mediterranean basin[8] represents a natural focus of interest for researchers and at the same time a natural laboratory for modeling and predicting climate change and its ecological effects. In particular, the increase in temperature is one of the greatest threats for corals, which can be considered as a probe of global warming effects, as it triggers bleaching events and widespread mortality.[9−11] Several recent mass mortality events of Mediterranean corals have been reported as being related to high temperatures.[12−16]

This study focuses on two scleractinian species of the Mediterranean Sea, already studied as a model for climate change: *Balanophyllia europaea* (Risso, 1826) and *Leptopsammia pruvoti* (Lacaze-Duthiers, 1897)[17] (Figure 1). *B. europaea* is a solitary, zooxanthellate (i.e., symbiotic with unicellular algae named zooxanthellae) coral, endemic to the Mediterranean Sea. Its distribution is limited to depths of 0−50 m because of its symbiosis with zooxanthellae, which require light.[17−19] *L.*

Received: November 12, 2012
Revised: September 13, 2013
Accepted: October 21, 2013
Published: October 21, 2013

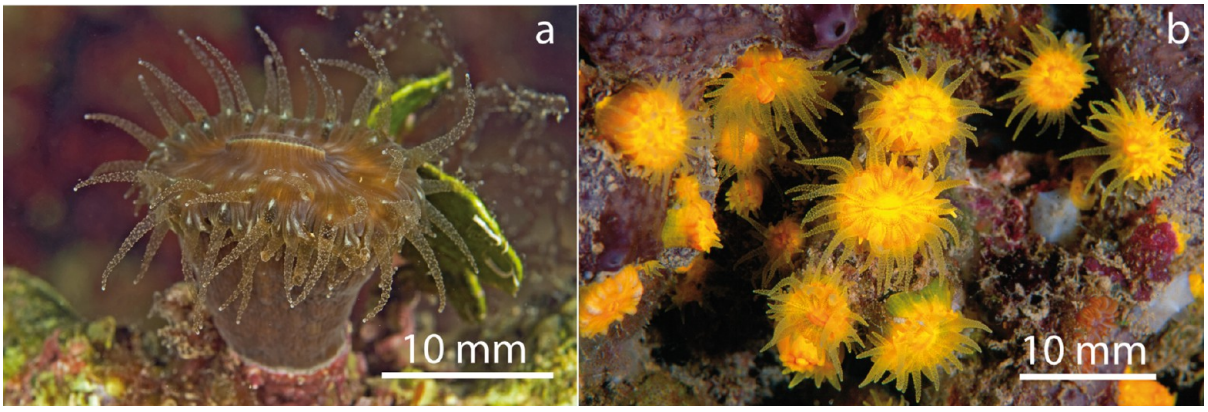

Figure 1. (a) Living polyp of *B. europaea* and (b) several living polyps of *L. pruvoti*.

pruvoti is a nonzooxanthellate and solitary scleractinian coral, distributed in the Mediterranean basin and along the European Atlantic coast from Portugal to Southern England and Ireland. Its distribution is limited to semienclosed rocky habitats, under overhangs, in caverns, and in small crevices, at depths of 0−70 m.[17,18] Corals were collected at three different Italian sites (see Figure 2), where the porosity of the two species has been

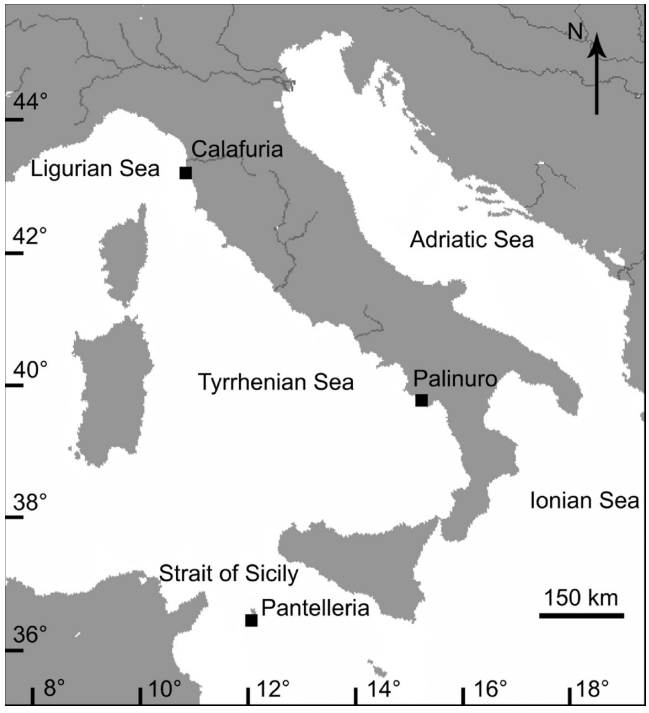

Figure 2. Map of the sites in Italy where corals were collected.

studied previously,[17] along a latitude and sea surface temperature (SST) gradient. Temperature, the variation of which is mainly influenced by latitude,[20] is linked to coral biometry, physiology, and demography.[21−23]

Coral Porosity and Pore-Size Distribution. The porosity (ratio of pore volume to sample volume) and pore-space structure of mineralized tissues are crucially important in determining overall properties and biological functions, such as the coral skeleton resistance to natural and anthropogenic breakage. They are important parameters for studying the growth of scleractinian corals and the effects of abiotic and anthropogenic influences on coral reefs.[24] Of additional interest is a good knowledge of the role of porosity in diagenesis.

The measured values of these parameters depend on the measurement methods[24,25] and can present spatial variations.[26] This could be the reason why their dependence on environmental conditions remains largely unstudied, notwithstanding their importance and their variation with factors such as exposure, temperature, latitude, depth, and species.

Recent investigations[17,19,27] have shown that along the Italian coast the porosity of *B. europaea* is positively correlated with SST. There is concern for the future of this species[17,27,28] in relation to the current predictions of global warming by the Intergovernmental Panel on Climate Change.[7] On the other hand, for *L. pruvoti*, both SST and solar radiation do not seem to influence significantly the porosity or space colonization potential.[17,19,29] An important aspect is the possible hierarchical structure of the porosity. Recently,[30] the flaw tolerance in nacre has been ascribed to the nanoparticle architecture of the aragonite platelet, which makes a crack propagate in an intergranular manner. The structure of porous media at different length scales is of great importance also in the use of corals as potential bone graft substitute material.[31]

Porosity and pore-size distributions can be investigated by many methods.[32−36] The results strongly depend on the physical principles adopted and on the assumptions of pore shape and connectivity (see the Supporting Information). Porosity and pore-size distributions determined by mercury intrusion porosimetry (MIP) for eight different coral species[36] showed large differences, with diameters ranging from 0.2 to 100 μm. However, it has been emphasized that particle compression and rupture can result from the high Hg pressure used. Time-domain nuclear magnetic resonance (TD-NMR)[37] has the advantage of being nondestructive and noninvasive. TD-NMR and in particular magnetic resonance relaxometry of ^{1}H nuclei of water saturating the pore space are efficient tools for investigating pore-space structure. Known since the 1950s,[38,39] and validated over time by comparison with MIP and, for specific surface, the Brunauer, Emmett, Teller (BET) method, it is now widely applied.[40−52] It is particularly useful for porous media with wide pore-sizes distributions, like those of corals. In this paper, the distributions of the local transverse relaxation time (T_2) of ^{1}H of water saturating the pore space of the cleaned coral skeletons, corresponding to distributions of "NMR pore sizes", are used (more details on NMR and surface effects in the Supporting Information). To the best of our

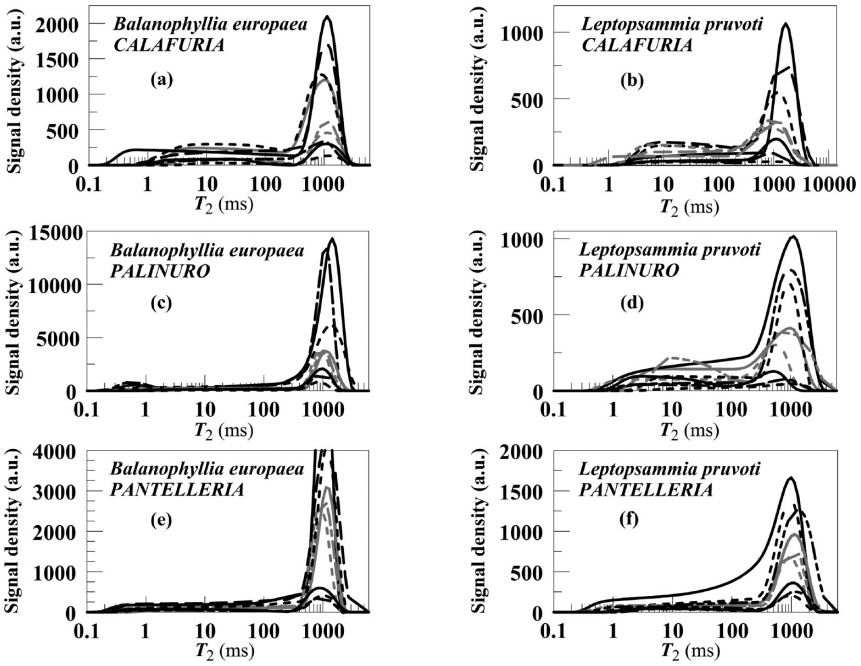

Figure 3. T_2 relaxation time distributions of the ^{1}H NMR signal from samples of cleaned skeletons of *B. europaea* (left) and *L. pruvoti* (right), after water saturation of the connected pore space. The samples were from three different sites. Distributions from all corals are represented (nine corals for each site). The sites were Calafuria (a and b), Palinuro (c and d), and Pantelleria (e and f). The total NMR signal (S_{NMR}) is represented by the area below each T_2 distribution and is proportional to the amount of water saturating the pore space and, therefore, to the volume of the connected pore space itself.

knowledge, this is the first time that this technique has been applied in this kind of investigation of corals.

MATERIALS AND METHODS

Corals. Specimens of *B. europaea* and *L. pruvoti* (54 specimens in all) were randomly collected from three sites: Calafuria (CL), Palinuro (PL), and Pantelleria Isle (PN) (see Figure 2). Coral tissue was totally removed, and corals were cleaned as described in ref 17. The skeletons were weighed to determine the mass (m). The total volume (V_T) was determined,[19] including the volume of the oral cavity. Then the specimens were saturated with water for NMR measurements. Further details are reported in the Supporting Information.

Total NMR Signal, Microporosity, and Cutoff Definitions. The total NMR signal (S_{NMR}), represented by the area below each T_2 distribution, is proportional to the volume of water saturating the pore-space volume (V_P). This signal divided by the total sample volume gives a value proportional to the total porosity of the specimen (see the Supporting Information). The fraction of water with relaxation times over a given interval of the distribution corresponds to the pore volume fraction over a corresponding pore-size range. "NMR microporosity", "microporosity" for short, will indicate the fraction of V_P where the smaller pores are weakly coupled by water diffusion to the large ones on the local relaxation time scale. This can be accomplished if the slope of the distribution shows a strong increase at a certain T_2 value, to be chosen as the point of separation between "smaller" and "larger" pores. This relaxation time will be called the "cutoff". The microporosity is then defined as the fraction of ^{1}H signal with a T_2 smaller than the cutoff, divided by the total ^{1}H signal. Operatively, it is the ratio of the area under the distribution for T_2 smaller than the cutoff to the total area under the distribution.

Statistical Analysis. Statistical analysis was performed using Statistical Package STATA 9.0 (StataCorp LP). To test the significance of the differences among species and growth sites, parametric and nonparametric tests were performed. Multivariate analyses were conducted using both ordinary least squares (OLS) robust to outliers and a nonparametric bootstrapping regression procedure following Efron,[53] applied to check the robustness of the results, that could be affected by small sample bias. The models are described by the function

$$y_i = a + b_1 m_i + b_2 \mathrm{SST}_i + \varepsilon_i \quad (1)$$

where index i refers to the n observations, y_i is the value of the dependent variable, and ε_i is the corresponding error. Parameters a and b_j (j = 1 or 2) are the best fit parameters, to be determined by OLS referring to the independent variables m and SST. More details can be found in the Supporting Information.

RESULTS AND DISCUSSION

Figure 3 shows the T_2 distributions of all *B. europaea* and *L. pruvoti* specimens. All the distributions show a main peak at long relaxation times and a long tail, with a smaller amplitude, ~3 orders of magnitudes wide. The major shape difference between the two species is the length of the tail. For *B. europaea* (panels a, c, and e), the tails go down to T_2 values of 0.1−0.2 ms, values shorter than those for *L. pruvoti* (panels b, d, and f). The principal differences among each group are given by the total areas and are due to the wide range of masses and volumes of the specimens. In principle, the ^{1}H signal can be produced by sources other than water, namely, the intraskeletal organic matrix, consisting of proteins, polysaccharides, and lipids. To check this possibility, T_2 distributions for a dry coral and the

same after complete water saturation were obtained and are shown in Figure 4. The discussion reported in the Supporting

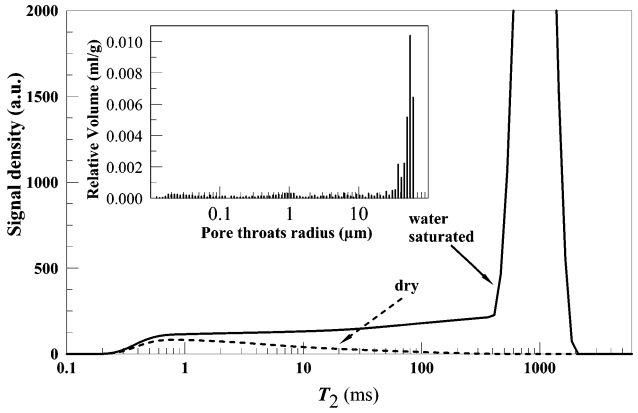

Figure 4. T_2 distribution of a dry coral (---) after 1 month in a desiccator and that of the same coral after full water saturation (—). In the inset, the MIP results for the same coral are shown. On the *x*-axis of the inset is given the pore throat radius distribution.

Information (referring to refs 54−61) leads us to conclude that in the distribution for the fully water saturated sample there is no contribution to the signal from macromolecular nuclei and only a maximum on the order of 2% could be attributed to lipids.

To discuss the distributions in Figure 3 in terms of pore sizes, one should get an approximate value for the radius of the pores inside the coral. The inset in Figure 4 reports the MIP distribution for the same specimen. The major fraction of the pore volume is given by pores whose entrance radii are on the order of tens of micrometers, while a minor fraction corresponds to a 3 order of magnitude long tail of very small pores, down to tens of nanometers. NMR and MIP results are exceptionally similar and consistent. The two classes of pores are easily distinguished also in the distributions in Figure 3, so that the two parameters microporosity and cutoff were determined for each distribution. The sharp boundary between the two classes, with a cutoff in the T_2 range of 200−400 ms, suggests that the two classes of pores are not well connected by water diffusion during a local relaxation time. Also, the long tail indicates that these pores are poorly connected both to the other small pores and to the large ones in the major class. On the basis of the comparison with MIP, microporosity should correspond to pore sizes in the range from ∼10 nm to ∼10−20 μm. The existence of a wide class of pores with sizes of less than 10−20 μm is described well in the SEM images of both species reported in Figure 5.

Table 1 lists means, standard errors, and statistical significances of the differences between the two species by both parametric and nonparametric tests for all the variables considered: microporosity, cutoff, mass, total volume, S_{NMR}, and S_{NMR}/V_T. The two species behave differently with a high degree of statistical significance ($p < 0.01$ for all variables, including NMR parameters). In particular, the mass and total volume for *B. europaea* are much larger than for *L. pruvoti*, and vice versa, the total porosity estimated by the ratio S_{NMR}/V_T is larger for *L. pruvoti* than for *B. europaea*. This result is consistent with the higher porosity obtained for *L. pruvoti* by previous non-NMR analysis,[17] where the difference was considered to be likely a consequence of the different habitats of the two species.

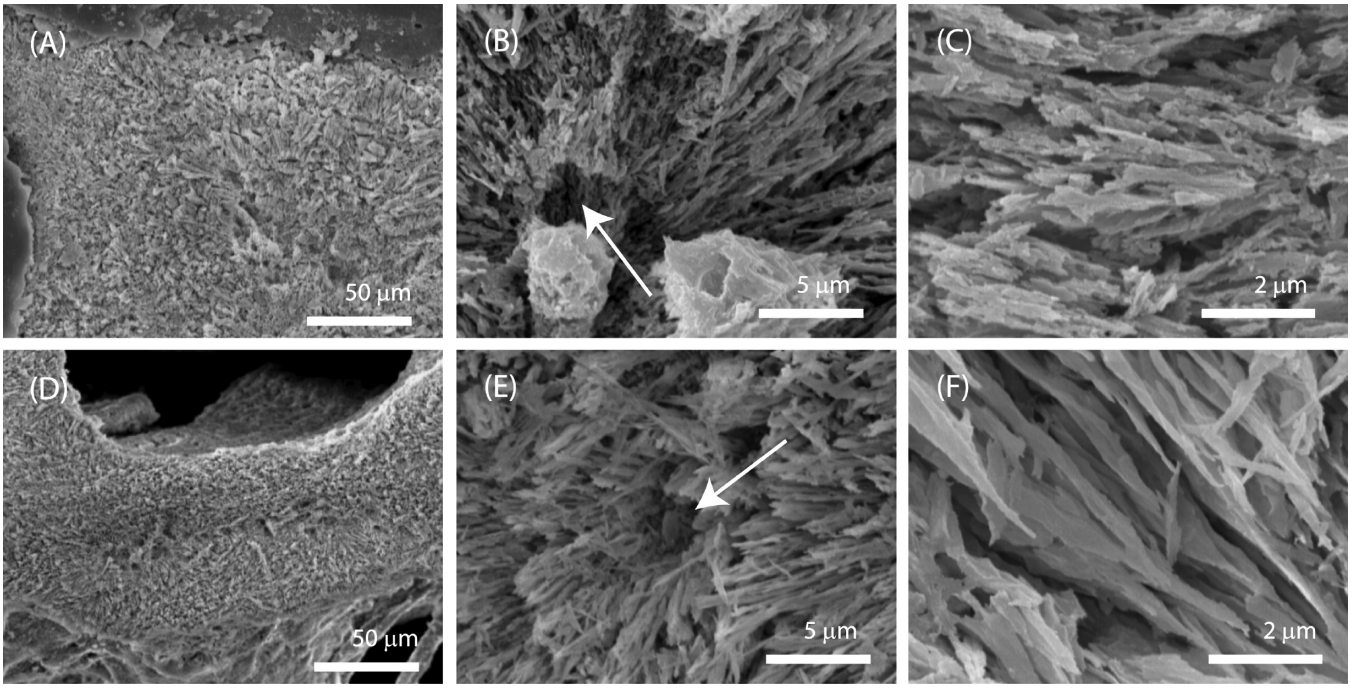

Figure 5. Scanning electron microscope pictures of a cross section of the tip region of a septum, the primary macroscopic structure of the coral skeleton, from *B. europaea* (A−C) and *L. pruvoti* (D−F). The building blocks of the skeleton are formed of thin aragonite crystals or fibers (0.04−0.05 μm in diameter), which form a three-dimensional structure. Their growth occurs in periodic layers and starts from the centers of calcification (see the arrows). The texture of the fibers of aragonite and the distribution of centers of calcification depend on the species of coral and are genetically controlled.

Table 1. Descriptive and Test Statistics Split by Species[a]

	B. europaea			*L. pruvoti*				
	n	mean	standard error	*n*	mean	standard error	*t*	*Z*
microporosity (%)	27	31.3	1.6	26	38.6	2.1	2.79	6.66
cutoff (ms)	27	337	15	26	249	20	3.59	12.92
m (g)	27	0.88	0.15	26	0.25	0.04	3.92	11.19
V_T (cm^3)	27	0.92	0.17	27	0.20	0.03	4.13	17.46
S_{NMR} (arbitrary units)	27	4060	820	27	1233	165	3.38	11.21
S_{NMR}/V_T (arbitrary units)	27	4800	275	27	6993	349	4.94	17.60

[a]Number of observations (*n*), means, standard errors, and statistical significances of differences in microporosity, cutoff, mass (*m*), total volume (V_T, including the oral cavity), NMR signal (S_{NMR}), and S_{NMR}/V_T for *B. europaea* and *L. pruvoti*. The values of the *t* test and *Z* test suggest a high degree of statistical significance ($p < 0.01$) between the two species for all the variables considered.

Table 2. Descriptive and Test Statistics of the Same Data in Table 1 Split by Site[a]

	CL			PL			PN				
	n	mean	standard error	*n*	mean	standard error	*n*	mean	standard error	*F*	χ^2
					(A) *B. europaea*						
microporosity	9	38.6	1.6	9	26.1	2.1	9	29.0	2.7	8.89[b]	11.83[b]
cutoff	9	283	18	9	361	23	9	367	28	3.98[c]	6.10[c]
m	9	0.42	0.11	9	1.3	0.3	9	0.9	0.3	3.35[d]	4.72[d]
V_T	9	0.4	0.1	9	1.5	0.4	9	0.9	0.2	3.39[d]	4.70[d]
S_{NMR}	9	1806	426	9	6990	1996	9	3382	792	4.42[c]	7.01[c]
S_{NMR}/V_T	9	4447	436	9	4860	301	9	5092	655	0.45	1.95
					(B) *L. pruvoti*						
microporosity	8	40.5	2.3	9	42.8	4.3	9	32.8	3.3	2.26	4.71[d]
cutoff	8	294	49	9	186	21	9	272	19	3.40[d]	6.88[c]
m	8	0.17	0.04	9	0.25	0.07	9	0.33	0.08	1.34	2.03
V_T	9	0.15	0.03	9	0.17	0.05	9	0.28	0.06	2.19	3.27
S_{NMR}	9	989	202	9	1090	246	9	1621	369	1.45	1.95
S_{NMR}/V_T	9	7700	729	9	7311	582	9	5967	334	2.53	4.17

[a]The sites are Calafuria (CL), Palinuro (PL), and Pantelleria (PN). The variables and units are the same as in Table 1. The values of the *F* test and χ^2 test suggest statistical significance of differences among the three sites for *B. europaea*. For *L. pruvoti*, only NMR parameters microporosity and cutoff show statistical significance, even if at a lower level. [b]$p < 0.01$. [c]$p < 0.05$. [d]$p < 0.1$.

Table 2 lists the differences in the means of the same species among growing sites. For *B. europaea*, the differences have a high degree of statistical significance for almost all variables. Microporosity has the highest degree of significance (microporosity, $p < 0.01$; cutoff, $p < 0.05$; mass and total volume, $p < 0.1$; S_{NMR}, $p < 0.05$). For *L. pruvoti*, only NMR parameters cutoff and microporosity show significant differences among sites ($p < 0.05$–0.1).

Table S1 of the Supporting Information lists the results of the correlation among variables performed separately for *B. europaea* (part A) and *L. pruvoti* (part B). For both species, pairs of variables, mass and total volume, mass and S_{NMR}, and total volume and S_{NMR}, are significantly correlated ($p < 0.01$). The correlations between microporosity and cutoff and between microporosity and mass are statistically significant for both species ($p < 0.01$ for *B. europaea*, and $p < 0.05$ for *L. pruvoti*).

Figure 6 reveals a counterintuitive behavior: the longer the cutoffs, the smaller the microporosities; at the first glance, one would expect the contrary. The pore-space architecture differs between samples with higher or lower cutoffs (between lower or higher microporosities). The scatter plots in Figure S2 of the Supporting Information and in Figure 7, showing cutoff versus mass and microporosity versus mass, respectively, suggest that the observed correlations between the cutoff and mass are governed by the mass: the smaller the mass, the higher the microporosity and the shorter the cutoff. As the mass of the corals increases, both the cutoff (which separates the two main pore classes) and the ratio between the fraction of the two pore classes change, with larger pores becoming more abundant. This effect is shown also by *L. pruvoti*, but it is not as marked as in *B. europaea* because of the smaller range of masses of corals. This is consistent with the gradual "filling up" of the smaller pores with the growth of the coral. A secondary infilling of skeletal pores in the older portion of the skeleton is a consistent characteristic of the skeletal density of branches of tall

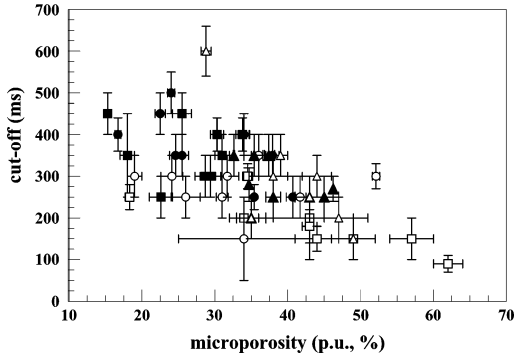

Figure 6. Scatter plot of the cutoff vs microporosity for all the samples. Filled symbols depict data for *B. europaea*, and empty symbols depict data for *L. pruvoti*. The symbols for the three sites are triangles (Calafuria), squares (Palinuro), and circles (Pantelleria).

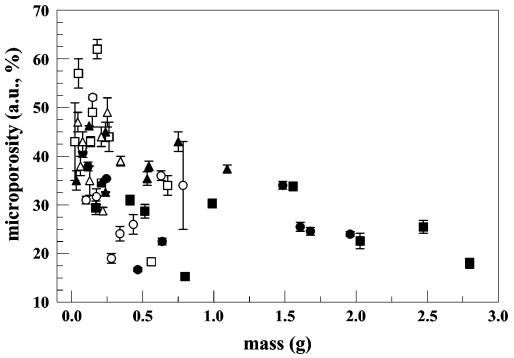

Figure 7. Scatter plot of microporosity vs mass for all the samples. Filled symbols depict data for *B. europaea*, and empty symbols depict data for *L. pruvoti*. The symbols of the three sites are triangles (Calafuria), squares (Palinuro), and circles (Pantelleria).

branching corals, in which growing tips are very porous while basal regions are extremely dense.[62]

To study how microporosity, considered a dependent variable, is affected by mass and SST, multiple-regression analysis was performed (eq 1) both for all the specimens and for the two species separately. Part A of Table 3 summarizes the results. First, it is important to observe that from a statistical point of view a potential correlation between m and SST does not invalidate the results, as all the values of the variance inflation factor (VIF) are $\ll$10. By considering all the specimens, the variable mass ($p < 0.01$) and SST ($p < 0.05$) significantly and negatively affect microporosity. In other words, the larger the mass and the higher the temperature, the smaller the microporosity. These relationships are mainly in place in the *B. europaea* species. For *L. pruvoti*, only the mass appears to be significantly related to the microporosity with a high degree of significance ($p < 0.05$). That means that SST appears to be a significant parameter in determining microporosity for *B. europaea* even if it is not as important as mass. The bootstrapping procedure (Table 3, part B) gives robustness to the evidence showing that those are not driven by small sample bias.

To better visualize and further discuss these relationships, the linear dependencies among microporosity, mass, and SST, for *L. pruvoti* and *B. europaea* separately, have been studied. Figure S3 of the Supporting Information lists the scatter plots and statistical significances. The results confirm the multivariate analysis. For both *L. pruvoti* and *B. europaea*, SST does not significantly affect mass, as the probability values of the slope of the linear best fit are not statistically significant ($p > 0.1$). Overall, the fact that the mass significantly affects microporosity at least at the 5% level emerges ($p < 0.05$ for *L. pruvoti*, and $p < 0.01$ for *B. europaea*). Results for microporosity versus SST show that a significant relationship exists for *B. europaea* ($p < 0.05$) but not for *L. pruvoti* ($p > 0.1$).

In a previous study,[17] it has been shown that porosity depends on temperature for *B. europaea*, but not for *L. pruvoti*. It has been hypothesized that the increase in porosity with temperature in the zooxanthellate species could depend on an inhibition of the photosynthetic process at elevated temperatures,[23,63] causing an attenuation of calcification[64] with possible negative consequences also for space colonization and population density.[19,27] The NMR results point in the same direction and seem to indicate also that this effect could be accompanied by a decrease in microporosity, meaning an increase in the fraction of the largest pores in the pore space.

TD-NMR is a quick, noninvasive, nondestructive method that does not use ionizing radiation, which can be applied to gain insight into the pore-space architecture of scleractinian corals, showing differences between species and growing sites, and sensitivity to environmental changes. Of course, this method, as well as MIP, BET, and the hydrostatic balance method, provides information about the connected porosity only and, as such, can be applied to systems with low fractions of isolated pores. This method can provide information that cannot be attained in other ways, like changes in the internal architecture of corals described by microporosity and cutoff with increasing mass and growing temperature. Even if this method cannot spatially locate the heterogeneity of the pore space, the existence of a clear cutoff in almost all the distributions (a very high slope at a certain point of the distribution) means that the smallest pores are not well connected by diffusion on the NMR time scale (corresponding to the local value of T_2) to the largest ones. Moreover, the NMR-defined parameter microporosity can quantify the ratio between the volume of the smallest pores (sizes of less than 10−20 μm) and the total pore volume.

The increased fraction of larger pores in the zooxanthellate corals with increasing SST values, which could reduce their

Table 3. Regression Analysis for Microporosity[a]

	(A) OLS			(B) bootstrap (5000 replications)		
	1	2	3	1	2	3
	all	*B. europaea*	*L. pruvoti*	all	*B. europaea*	*L. pruvoti*
m (g)	−7.19[b] (−5.86)	−4.69[b] (−3.28)	−21.04[c] (−2.32)	−6.88[b] (−4.69)	−5.57[b] (−3.72)	−22.47[d] (−1.79)
SST (°C)	−3.53[c] (−2.41)	−4.06[c] (−2.11)	−2.53 (−0.96)	−3.53[c] (−2.38)	−3.34[d] (−1.76)	−2.76 (−0.99)
constant	108.6[b] (3.85)	115.5[b] (3.12)	94.0[d] (1.85)	107.2[b] (3.70)	108.3[b] (2.95)	101.4[d] (1.77)
mean VIF (maximum)	1.22 (1.33)	1.20 (1.24)	1.34 (1.43)			
no. of observations	53	27	26	53	27	26
R^2 adjusted	0.32	0.41	0.24	0.32	0.38	0.24
F test	30.7[b]	15.8[b]	4.7[c]			
Wald χ^2				43.2[b]	37.0[b]	6.2

[a]OLS robust to outliers (robust t statistics in parentheses) and bootstrap (values of bootstrapped Z test in parentheses). (1) All specimens, (2) *B. europaea*, and (3) *L. pruvoti*. The coefficients in the columns are the parameters b_j (j = 1 or 2) and the parameter a (constant) of eq 1, where y_i is the value of the microporosity for each observation considered. Values of VIF of $\ll$10 indicate that a possible correlation between m and SST does not invalidate the results. [b]$p < 0.01$. [c]$p < 0.05$. [d]$p < 0.1$.

resistance to mechanical stresses, could have particular consequences in determining the effects of global warming on these species.[65] The described method will be applied in future work to the effects of ocean acidification on the skeletal properties of corals[66] and other calcifying organisms.

■ ASSOCIATED CONTENT

Supporting Information

Additional observations and data (all reference numbers refer to the reference list in the main text). This material is available free of charge via the Internet at http://pubs.acs.org.

■ AUTHOR INFORMATION

Corresponding Author

*Telephone: +390512095119. Fax: +390512095047. E-mail: paola.fantazzini@unibo.it.

Notes

The authors declare no competing financial interest.

■ ACKNOWLEDGMENTS

This research has received funding from the European Research Council under the European Union's Seventh Framework Programme (FP7/2007-2013)/ERC Grant 249930 (Coral-Warm: Corals and global warming: the Mediterranean versus the Red Sea). We thank F. Gizzi, C. Marchini, and S. Prantoni for help in collecting the samples, the diving centers Centro Immersioni Pantelleria and Il Pesciolino for logistic assistance in the field, the Scientific Diving School for collaboration in the underwater activities, Fausto Peddis for MIP measurements, Gianni Neto for pictures of living specimens, and Robert James Sidford Brown for carefully reading the manuscript.

■ REFERENCES

(1) Stenseth, N. H. Ecological effects of climate fluctuations. *Science* **2002**, *297*, 1292−1296.

(2) Karl, T. R.; Trenberth, K. E. Modern global climate change. *Science* **2003**, *302*, 1175−1177.

(3) Parmesan, C. Ecological and evolutionary responses to recent climate change. *Annual Review of Ecology and Systematics* **2006**, *37*, 637−669.

(4) Helmuth, B.; Mieszkowska, N.; Moore, P.; Hawkins, S. J. Living on the edge of two changing worlds: Forecasting the responses of rocky intertidal ecosystems to climate change. *Annual Review of Ecology and Systematics* **2006**, *37*, 373−404.

(5) Harley, C. D. G.; Hughes, A. R.; Hultgren, K. M.; Miner, B. G.; Sorte, C. J. B.; Thornber, C. S.; Rodriguez, L. F.; Tomanek, L.; Williams, S. L. The impacts of climate change in a coastal marine systems. *Ecology Letters* **2006**, *9*, 228−241.

(6) Richardson, A. J.; Poloczanska, S. Under-resourced, under threat. *Science* **2008**, *320*, 1294−1295.

(7) Solomon, S.; Qin, D.; Manning, M.; Marquis, M.; Averyt, K.; Tignor, M. M. B.; Le Roy Miller, H., Jr.; Chen, Z. Climate Change 2007: The Physical Science Basis. Contribution of Working Group I to the Fourth Assessment Report of the Intergovernmental Panel on Climate Change. Cambridge University Press: Cambridge, U.K., 2007.

(8) Lejeusne, C.; Chevaldonné, P.; Pergent-Martini, C.; Boudouresque, C. F.; Pérez, T. Climate change effects on a miniature ocean: The highly diverse, highly impacted Mediterranean Sea. *Trends in Ecology & Evolution* **2010**, *25*, 250−260.

(9) Hughes, T. P.; Baird, A. H.; Bellwood, D. R.; Card, M.; Connolly, S. R.; Folke, C.; Grosberg, R.; Hoegh-Guldberg, O.; Jackson, J. B. C.; Kleypas, J.; Lough, J. M.; Marshall, P.; Nyström, M.; Palumbi, S. R.; Pandolfi, J. M.; Rosen, B.; Roughgarden, J. Climate change, human impacts, and the resilience of coral reefs. *Nature* **2003**, *301*, 929−933.

(10) Hoegh-Guldberg, O. The impact of Climate Change on Coral Reef Ecosystems. In *Coral Reefs: An Ecosystem in Transition*; Dubinsky, Z., and Stambler, N., Eds.; Springer: Dordrecht, The Netherlands, 2011; pp 391−404.

(11) Lesser, M. Coral Bleaching: Causes and Mechanisms. In *Coral Reefs: An Ecosystem in Transition*; Dubinsky, Z., and Stambler, N., Eds.; Springer: Dordrecht, The Netherlands, 2011; pp 405−420.

(12) Cerrano, C.; Bavestrello, G.; Bianchi, C. N.; Cattaneo-Vietti, R.; Bava, S.; Morganti, C.; Morri, C.; Picco, P.; Sara, G.; Schiaparelli, S.; Siccardi, A.; Sponga, F. A catastrophic mass-mortality episode of gorgonians and other organisms in the Ligurian Sea (North-Western Mediterranean), summer 1999. *Ecology Letters* **2000**, *3*, 284−293.

(13) Perez, T.; Garrabou, J.; Sartoretto, S.; Harmelin, J. G.; Francour, P.; et al. Mass mortality of marine invertebrates: An unprecedented event in the Northwestern Mediterranean. *C. R. Acad. Sci., Ser. III* **2000**, *323*, 853−865.

(14) Rodolfo-Metalpa, R.; Bianchi, C. N.; Peirano, A.; Morri, C. Coral mortality in NW Mediterranean. *Coral Reefs* **2000**, *19*, 24.

(15) Coma, R.; Ribes, M.; Serrano, E.; Jimenez, E.; Salat, J.; Pasqual, J. Global warming-enhanced stratification and mass mortality events in the Mediterranean. *Proc. Natl. Acad. Sci. U.S.A.* **2009**, *106*, 6176−6181.

(16) Garrabou, J.; Coma, R.; Bensoussan, N.; Bally, M.; Chevaldonne, P.; Cigliano, M.; Diaz, D.; Harmelin, J. G.; Gambi, M. C.; Kersting, D. K.; Ledoux, J. B.; Lejeusne, C.; Linares, C.; Marschal, C.; Perez, T.; Ribes, M.; Romano, J. C.; Serrano, E.; Teixido, N.; Torrents, O.; Zabala, M.; Zuberer, F.; Cerrano, C. Mass mortality in the NW Mediterranean rocky benthic communities: Effects of the 2003 heat wave. *Global Change Biology* **2009**, *15*, 1090−1103.

(17) Caroselli, E.; Prada, F.; Pasquini, L.; Nonnis Marzano, F.; Zaccanti, F.; Falini, G.; Levy, O.; Dubinsky, Z.; Goffredo, S. Environmental implications of skeletal micro-density and porosity variation in two scleractinian corals. *Zoology* **2011**, *114*, 255−264.

(18) Zibrowius, H. *The scleractinians of the Mediterranean and of the North-Eastern Atlantic*; Memorial Institute of Oceanography, 1980; Vol. *11*, pp 1−284.

(19) Goffredo, S.; Caroselli, E.; Mattioli, G.; Pignotti, E.; Zaccanti, F. Variation in biometry and demography of solitary corals with environmental factors in the Mediterranean Sea. *Mar. Biol.* **2007**, *152*, 351−361.

(20) Kain, J. M. The seasons in the subtidal. *British Phycological Journal* **1989**, *24*, 203−215.

(21) Kleypas, J. A.; McManus, J. W.; Menez, L. A. B. Environmental limits to coral reef development: Where do we draw the line? *Am. Zool.* **1999**, *39*, 146−159.

(22) Lough, J. M.; Barnes, D. J. Environmental controls on growth of the massive coral *Porites*. *J. Exp. Mar. Biol. Ecol.* **2000**, *245*, 225−243.

(23) Al-Horani, F. A. Effects of changing seawater temperature on photosynthesis and calcification in the scleractinian coral *Galaxea fascicularis*, measured with O_2, Ca^{2+} and pH microsensors. *Sci. Mar.* **2005**, *69*, 347−354.

(24) Roche, R. C.; Abel, R. A.; Johnson, K. G.; Perry, C. T. Quantification of porosity in *Acropora pulchra* (Brook 1891) using X-ray micro-computed tomography techniques. *J. Exp. Mar. Biol. Ecol.* **2010**, *396*, 1−9.

(25) Bucher, D. J.; Harriott, V. J.; Roberts, L. G. Skeletal micro-density, porosity and bulk density of acroporid corals. *J. Exp. Mar. Biol. Ecol.* **1998**, *228*, 117−136.

(26) Roche, R. C.; Abel, R. L.; Johnson, K. G. Spatial variation in porosity and skeletal element characteristics in apical tips of the branching coral *Acropora pulchra* (Book 1891). *Coral Reefs* **2011**, *30*, 195−201.

(27) Goffredo, S.; Caroselli, E.; Mattioli, G.; Pignotti, E.; Dubinsky, Z.; Zaccanti, F. Inferred level of calcification decreases along an increasing temperature gradient in a Mediterranean endemic coral. *Limnol. Oceanogr.* **2009**, *54*, 930−937.

(28) Goffredo, S.; Caroselli, E.; Mattioli, G.; Pignotti, E.; Zaccanti, F. Relationships between growth, population structure and sea surface temperature in the temperate solitary coral *Balanophyllia europaea* (Scleractinia, Dendrophylliidae). *Coral Reefs* **2008**, *27*, 623−632.

(29) Caroselli, E.; Zaccanti, F.; Mattioli, G.; Falini, G.; Levy, O.; Dubinsky, Z.; Goffredo, S. Growth and demography of the solitary scleractinian coral *Leptopsammia pruvoti* along a sea surface temperature gradient in the Mediterranean Sea. *PLoS One* **2012**, *7*, e37848.
(30) Huang, Z.; Li, X. Origin of flaw-tolerance in nacre. *Sci. Rep.* **2013**, *3*, 1693.
(31) Nomura, T.; Katz, J. L.; Powers, M. P.; Saito, C. Evaluation of the micromechanical elastic properties of potential bone-grafting materials. *J. Biomed. Mater. Res., Part B* **2005**, *73*, 29−34.
(32) Espinal, L. Porosity and its measurement. In *Characterization of Materials*; John Wiley and Sons: New York, 2012 (Wiley online library, published online June 25, 2012).
(33) Klobes, P.; Meyer, K.; Munro, R. G. Porosity and specific surface area measurements for solid materials. In *Recommanded Practice Guide*; Special Publication 960-17; National Institute of Standards and Technology: Gaithersburg, MD, 2006.
(34) Sing, K. The use of nitrogen adsorption for the characterization of porous materials. *Colloids Surf., A* **2001**, *187*−*188*, 3−9.
(35) Stapf, S., Han, S.-I., Eds. *NMR imaging in chemical engineering*; Wiley-VCH Verlag GmbH & Co. KGa: Weinheim, Germany, 2006.
(36) Laine, J.; Labady, M.; Albornoz, A.; Yunes, S. Porosities and pore sizes in coralline calcium carbonate. *Mater. Charact.* **2008**, *59*, 1522−1525.
(37) Cowan, B. *Nuclear Magnetic Resonance and Relaxation*; Cambridge University Press: Cambridge, U.K., 1997.
(38) Brown, R. J. S. Measurements of nuclear spin relaxation of fluids in bulk for large surface-to-volume ratios. *Bulletin of the American Physics Society, Series II* **1956**, *1*, 216.
(39) Brown, R. J. S. Nuclear magnetism logging at the Coyote institute. *Magn. Reson. Imaging* **1996**, *14*, 811−817.
(40) Brownstein, K. R.; Tarr, C. E. Importance of classical diffusion in NMR studies of water in biological cells. *Phys. Rev. A* **1979**, *19*, 2446−2453.
(41) D'Orazio, F.; Tarczon, J. C.; Halperin, W. P. Application of nuclear magnetic resonance pore structure analysis to porous silica glass. *J. Appl. Phys.* **1989**, *65*, 742−751.
(42) Fantazzini, P., Bortolotti, V., Kärger, J., Galvosas, P., Eds. *Conference Proceedings Series 1330*; American Institute of Physics: College Park, MD, 2011.
(43) Borgia, G. C.; Brancolini, A.; Brown, R. J. S.; Fantazzini, P.; Ragazzini, G. Water-air saturation changes in restricted geometries studied by proton relaxation. *Magn. Reson. Imaging* **1994**, *12*, 191−195.
(44) Borgia, G. C.; Brown, R. J. S.; Fantazzini, P.; Mesini, E.; Valdré, G. Diffusion weighted spatial information from ^{1}H relaxation in restricted geometries. *Il Nuovo Cimento* **1992**, *14D*, 745−759.
(45) Dunn, K.-J.; Bergman, D. J.; Latorraca, G. A. *Nuclear magnetic resonance petrophysical and logging applications*; Pergamon: New York, 2002.
(46) Hirasaki, G. J. NMR applications in Petroleum Reservoir Studies. In *NMR Imaging in Chemical Engineering*; Stapf, S., and Han, S.-I., Eds.; Wiley-VCH Verlag GmbH & Co. KGaA: Weinheim, Germany, 2006; pp 321−340.
(47) Kleinberg, R. L. Utility of NMR T_2 distributions, connection with capillary pressure, clay effect, and determination of the surface relaxivity parameter ρ_2. *Magn. Reson. Imaging* **1996**, *14*, 761−767.
(48) Borgia, G. C.; Brown, R. J. S.; Fantazzini, P. Nuclear magnetic resonance relaxivity and surface-to-volume ratio in porous media with a wide distribution of pore sizes. *J. Appl. Phys.* **1996**, *79*, 3656−3664.
(49) Brai, M.; Casieri, C.; De Luca, F.; Fantazzini, P.; Gombia, M.; Terenzi, C. Validity of NMR pore-size analysis of cultural heritage ancient building materials containing magnetic impurities. *Solid State Nucl. Magn. Reson.* **2007**, *32*, 129−135.
(50) Borgia, G. C.; Brown, R. J. S.; Fantazzini, P. Examples of marginal resolution of NMR relaxation peaks using UPEN and diagnostics. *Magn. Reson. Imaging* **2001**, *19*, 473−475.
(51) Fantazzini, P.; Brown, R. J. S. Units in distributions of relaxation times. *Concepts Magn. Reson.* **2005**, *27A*, 122−123.
(52) Bortolotti, V.; Brown, R. J. S.; Fantazzini, P. *UpenWin: A software to invert multi-exponential decay data* (www.unibo.it/Portale/Ricerca/Servisi+Imprese/UpenWin.htm).
(53) Efron, B. Bootstrap methods: Another look to the Jackknife. *Annals of Statistics* **1979**, *7*, 1−26.
(54) Goffredo, S.; Vergni, P.; Reggi, M.; Caroselli, E.; Sparla, F.; Levy, O.; Dubinsky, Z.; Falini, G. The skeletal organic matrix from Mediterranean coral *Balanophyllia europaea* influences calcium carbonate precipitation. *PLoS One* **2011**, *6*, e22338.
(55) Fantazzini, P.; Galassi, F.; Bortolotti, V.; Brown, R. J. S.; Vittur, F. The search for negative amplitude components in quasi-continuos distributions of relaxation times: The example of ^{1}H magnetization exchange in articular cartilage and hydrated collagen. *New J. Phys.* **2011**, *13*, 065007.
(56) Liimatainen, T. J.; Ylä-Herttuala, S.; Hakumäki, J. M. ^{1}H NMR Spectroscopy study of lipid T1 and T2 Relaxation in BT4C rat gliomas in vivo. *Proceedings of the International Society of Magnetic Resonance Medicine* **2004**, *11*, 610.
(57) Rakow-Penner, R.; Daniel, B.; Yu, H.; Sawyer-Glover, A.; Glover, G. H. Relaxation times of breast tissue at 1.5T and 3T measured using IDEAL. *J. Magn. Reson. Imaging* **2006**, *23*, 87−91.
(58) Sehy, J. V.; Ackerman, J. J. H.; Neil, J. J. J. Water and lipid MRI of the *Xenopus* oocyte. *Magn. Reson. Med.* **2001**, *46*, 900−906.
(59) Opstad, K. S.; Griffiths, J. R.; Bell, B. A.; Howe, F. A. Apparent T2 relaxation times of lipid and macromolecules: A study of high-grade tumor spectra. *J. Magn. Reson. Imaging* **2008**, *27*, 178−184.
(60) Gambarota, G.; Tanner, M.; van der Graat, M.; Mulkern, R.; Newbould, R. D. Fast T2 relaxometry in ^{1}H-MRS of hepatic water and fat using shirt TR at 3T. *Proceedings of the International Society of Magnetic Resonance Medicine* **2004**, *19*, 2997.
(61) Bortolotti, V.; Fantazzini, P.; Gombia, M.; Greco, D.; Rinaldin, G.; Sykora, S. PERFIDI filters to suppress and/or quantify relaxation time components in multicomponent systems: An example for fat-water systems. *J. Magn. Reson.* **2010**, *206*, 219−226.
(62) Hughes, T. P. Skeletal density and growth form of corals. *Mar. Ecol.: Prog. Ser.* **1987**, *35*, 259−266.
(63) Jokiel, P. L.; Coles, S. L. Response of Hawaiian and other Indo-Pacific reef corals to elevated temperature. *Coral Reefs* **1990**, *4*, 155−162.
(64) Al-Horani, F. A.; Ferdelman, T.; Al-Moghrabi, S. M.; De Beer, D. Spatial distribution of calcification and photosynthesis in the scleractinian coral *Galaxea fascicularis*. *Coral Reefs* **2005**, *24*, 173−180.
(65) Madin, J. S.; Hughes, T. P.; Connolly, S. R. Calcification, storm damage and population resilience of tabular corals under climate change. *PLoS One* **2012**, *7*, e46637.
(66) Reyes-Nivia, C.; Diaz-Pulido, G.; Kline, D.; Hoegh-Guldberg, O.; Dove, S. Ocean acidifcation and warming scenarios increase microbioerosion of coral skeletons. *Global Change Biology* **2013**, *19*, 1919−1929.